CRISPR/Cas-based precision gene replacement in plants via homologous recombination-independent approaches

Tien Van Vu[1,2,*], Gah-Hyun Lim[3,4], Seung Hee Choi[4], Ju Yeon Moon[4], Ngan Thi Nguyen[1], Swati Das[1], Mil Thi Tran[1], Yeon Woo Sung[1], Jihae Kim[1], Young Jong Song[1], Suk Weon Kim[4], Jae Cheol Jeong[4], Jae-Yean Kim[1,5,*]

[1]Division of Applied Life Science (BK21 FOUR Program), Plant Molecular Biology and Biotechnology Research Center, Gyeongsang National University, Jinju 660-701, Republic of Korea.

[2]National Key Laboratory for Plant Cell Biotechnology, Agricultural Genetics Institute, Km 02, Pham Van Dong Road, Co Nhue 1, Bac Tu Liem, Hanoi 11917, Vietnam.

[3]Department of Biological Sciences, Pusan National University, Busan 46241, Republic of Korea

[4]Biological Resource Center, Korea Research Institute of Bioscience and Biotechnology (KRIBB), Jeongeup, 56212, Republic of Korea

[5]Nulla Bio Inc 501 Jinju-daero, Jinju 52828, Republic of Korea.

*Correspondence: Tien Van Vu: tienvu.agi@gmail.com (ORCID: 0000-0002-6369-7664). Jae-Yean Kim: kimjy@gnu.ac.kr (ORCID ID : 0000-0002-1180-6232).

Keywords: MMEJ, Precision gene editing, Microhomology, CRISPR/Cas, DNA repair, PITCh

Running title: HR-independent precise allele replacement.

Word count:

Introductory paragraph: 68/70

Main text: 1351 words.

References: 386 words.

Figure legends: 412 words.

Number of Main Figures: 02

Number of Supplementary Figures: 10

Number of Supplementary Tables: 12

Precision gene editing has been recently achieved by homology-directed gene targeting (HGT) and prime editing (PE), but implementation remains challenging in plants. Here, we report a novel tool for precision genome editing in plants employing microhomology-mediated end joining (MMEJ). The MMEJ-mediated precise gene replacement produced much higher targeted editing efficiencies than the cNHEJ, up to 8.89 %, 4.47 %, and 8.98 % in tomato, lettuce, and cabbage, respectively.

cNHEJ and MMEJ mechanisms were used for CRISPR/Cas9-based genome editing at high efficiency and specificity[1-3]. However, a system using cNHEJ and MMEJ for precise gene replacement has not been developed in plants. Here, we proposed and evaluated a novel MMEJ-based system for precise gene replacement (Supplementary Fig. 1 and 2a,b)[4]. A predefined genomic site with a protospacer adjacent motif (PAM) is determined first, thus enabling the prediction of the DSB formation site. The sequence between the two predicted cut sites is employed as a donor template so that its DNA sequence is essentially modified allowing it to carry targeted base changes to avoid recurrent cuts after gene replacement (Supplementary Fig. 2a,b). In the case of MMEJ-mediated editing, the predicted flanking DSB ends would then be used to choose microhomologies (MH1, and MH2, Supplementary Fig. 1b).

We employed PEG-mediated tomato protoplast transfection to deliver the SpCas9 proteins, gRNAs, and donors for replacing six base pairs of the exon 5 of SlHPAT3 (Fig. 1a,b; Supplementary Table 1 and Supplementary file 1). Targeted deep-sequencing data revealed editing efficiency as high as 2.46 % and 0.09% (Supplementary Fig. 2c and Supplementary Table 3) with the MJ.HPAT3-1 and cNJ.HPAT3-1 donor. Significantly, the edited products of the cNHEJ donor did not include base changes located at its two ends (Supplementary Tables 2 and 3). Further analysis of the edited products revealed multiple repaired products by the

MJ.HPAT3-1 donor with various frequencies (Fig. 1b). The precisely edited allele that contains all the intended base modification only accounted for 9.72 % of total edited reads (Supplementary Table 3). However, when we observed all the edited products containing the targeted B and C base changes, and excluded the others containing one-sided base changes (A1 and A2 or D1 and D2) that were designed to prohibit the recurrent cleavages of the SpCas9, we obtained a total of 805 reads corresponding to 33.01% of the total edited sequences (Fig. 1b; Supplementary Table 3). Our data also confirmed the simultaneous cutting activities of the gR1.HPAT3 and gR2.HPAT3 since most of the indel alleles were revealed with the traces of both the gRNA cleavages at the 3rd base upstream of PAM sequences (Fig 1a and Supplementary Figs. 4,5).

We next sought to investigate the implications of different donor doses on the frequency of MMEJ-mediated DNA replacement. The MMEJ-mediated editing frequencies with all base changes were increased with higher amounts of donor DNA, from 10.42 % (50 pmol) to 19.84 % (300 pmol), and the one-sided repair frequencies were reduced accordingly (Supplementary Fig. 6 and Supplementary Table 4). Moreover, when the MJ.HPAT3-1 donor dose was increased, the portions of targeted products (containing B and C base changes) were not different between 50 and 100 pmol but increased at higher doses, from 31.38 % (50 pmol) to 47.81 % (300 pmol) (Supplementary Table 4-5). In the case of the cNJ.HPAT3-1 donor, the editing efficiency did not vary much among the donor doses and was much lower compared to that of the MJ.HPAT3-1 (Fig. 1c). Again, most of its products contained only B and C changes (Supplementary Fig. 6).

Effective microhomology lengths (8-20 bases) increased MMEJ-mediated gene insertion in mammalian cells[1, 5, 6]. When the microhomology was shorter than 20 bp, the total editing efficiency was significantly reduced from 4.22 ± 0.47 % (MJ.HPAT3-1) to 2.33 ± 0.31 %

(MJ.HPAT3-2) and 2.65 ± 0.58 % (MJ.HPAT3-3) (Fig. 1d and Supplementary Table 6). More importantly, the all-base-change precise editing efficiency was significantly higher for 20-bp microhomology (0.28 ± 0.05 %) compared to that of the 10-bp (0.12 ± 0.03 %) and 5-bp (0.04 ± 0.01 %) microhomology lengths (Supplementary Table 6). Furthermore, when we consider all the reads containing the targeted base changes (B and C), the targeted editing efficiency was 1.16 ± 0.09; 0.66 ± 0.12; and 0.55 ± 0.06 % for the 20-bp; 10-bp; and 5-bp microhomologies, respectively. Interestingly, the activities of the gRNAs were not significantly different among all the treatments (Supplementary Table 6), indicating that the MMEJ-mediated editing efficiency obtained from the experiments depended on microhomology length[5-7].

We next tested if NU7441, a small chemical that was shown to significantly enhance the MMEJ-mediated DSB repair products in mammalian cells[8], can facilitate MMEJ repair. When the NU7441 concentration was increased from 0 to 1 μM, the editing efficiency was dramatically elevated in all the donors (Fig. 1e,f). The case of the MJ.HPAT3-2 donor was remarkable in that the precise editing efficiency was enhanced 23.9 folds, from 0.14 to 3.34 %, with 1μM of NU7441, similar to the highest MMEJ-mediated efficiency of MJ.HPAT3-1 (3.80%) under the same conditions (Fig. 1f and Supplementary Table 7). Moreover, the ratio of the repaired products containing only B and C base changes was dramatically increased with higher NU7441 concentrations, reaching up to 5.24 % at 1 μM of NU7441 in the case of the MJ.HPAT3-2 (Fig. 1e, f). To further check whether NU7441 negatively impacts the suspected cNHEJ-mediated DSB repair in the case of cNJ.HPAT3-1 donor, we conducted editing experiments using a cNJ.HPAT3-1 donor with the addition of 0.5, 1.0, and 2.0 μM of NU7441. Surprisingly, the editing efficiency gradually increased with the increment of NU7441 concentration, and most of the repaired products contained only B and C base changes. The editing efficiency reached

1.58 % when 2.0 µM of NU7441 was added (Fig. 1f), which is 1.88-fold higher than the treatment without NU7441.

The plant regeneration system for tomato protoplast was shown to be of very low efficiency and time-consuming. To overcome this challenge, we attempted to deliver the cNHEJ and MMEJ-mediated gene editing into a tomato by the *Agrobacterium*-mediated method[9]. SlHPAT3 and SlHKT1;2 loci were selected for editing via the cNHEJ and MMEJ approaches (Supplementary Fig. 7a,b and Supplementary file 1). Unexpectedly, the cNHEJ and MMEJ-mediated editing were extremely low at both the loci (Supplementary Table 8), possibly due to the low donor availability, the requirement of four simultaneous cleavages, and the nucleolytic damages to the unprotected ends of donors. The editing reads were mostly with one-side editing (Supplementary Fig. 8a) or one-sided insertion of the MMEJ donor (Supplementary Fig. 8b). However, subsequent screening of regenerated plants carried precisely edited alleles, albeit their editing rate was relatively low (up to 4% for the cNHEJ event cNJ1 and 3% for the MMEJ event #MJ5) (Supplementary Fig. 9).

To extend MMEJ-mediated precision gene editing to other plant species, we conducted MMEJ-mediated precise gene replacement in lettuce and cabbage using the RNP transfection method. The *THERMO-TOLERANCE 1* (*TT1*)[10], *ORANGE* (*Or*)[11, 12], and *ACETOLACTATE SYNTHASE 1* (*ALS1*)[13] genes were selected as targets for both lettuce and cabbage were identified by NCBI Blastp (Supplementary Fig. 10 and Supplementary Tables 9,10). We designed and employed two gRNAs for cutting genomic loci and MMEJ donors containing 20-base microhomologies at two ends (Fig. 2a,b). In lettuce, the highest MMEJ-mediated precise editing efficiency for all the intended base changes was 1.81 ± 0.75 % for the *LsALS1* locus, and the lowest efficiency was zero for the *LsTT1* locus. The *LsOr* locus showed only 0.13 ± 0.10 % for the exchange of all the

intended bases (Fig. 2c and Supplementary Table 11). Considering all the repaired products that contain the targeted base changes for the desirable a.a., the efficiency reached 4.47 %, 0.78%, and 0.42% for LsALS1, LsTT1, and LsOr locus, respectively (Fig 2c and Supplementary Table 11). In cabbage, the highest precise editing efficiency (7.27 ± 4.46 %) was obtained at the BoTT1 locus and lower at the BoOr gene (1.68 ± 0.24 %). The ALS1 locus for cabbage resulted in the least precise editing efficiency, at only 0.73 ± 0.43 %, nearly half of the editing efficiency obtained with the LsALS1 (Fig. 2d and Supplementary Table 12). The data from lettuce and cabbage indicate that MMEJ-mediated precision editing could be successfully extended to other plant species.

Taken together, we successfully engineered the error-prone MMEJ-mediated DSB repair mechanism for precision gene replacement in plants. However, it requires further optimization of efficiency, especially that of plant regeneration from the edited cells. This report offers another precision gene-editing tool that may help to advance crop breeding in the future.

Methods

Targeted genes and donor DNA preparation for RNP works. A tomato homolog of *Arabidopsis* hydroxyproline O-arabinosyltransferase 3 (SlHPAT3, accession no. Solyc07g021170.1) was chosen as the first target thanks to its highly active guide RNA (gRNA) pair[14]. We employed PEG-mediated tomato protoplast transfection experiments using RNPs with SpCas9 protein and two sgRNAs, gR1.HPAT3 and gR2.HPAT3 (Fig. 1a) for cutting the genomic sites, combining that with a chemically modified cNHEJ (cNJ.HPAT-1) donor or an MMEJ donor (MJ.HPAT3-1) (Supplementary Table 1 and Supplementary file 1) for the replacement of six base pairs of the exon 5 of SlHPAT3 (Fig. 1a). The 5’ end modified cNJ.HPAT3-1 was prepared by PCRs using 5’ modified oligos (5’ phosphorylated, phosphorothioate bond addition to the phosphodiester linkage between the first and the second nucleotides) (Supplementary

Table 1) synthesized by Bioneer (Korea) without a template. The MMEJ donors were prepared by PCRs using oligos (Supplementary Table 1) synthesized by Bioneer (Korea) without templates. A high-fidelity DNA Taq polymerase was used for the PCR amplifications. The PCR products were cleaned using a BIOFACT PCR cleanup kit (BIOFACT, Korea). The donor concentrations were assessed by Nanodrop2000 spectrophotometer (Thermofisher, USA) and directly used for transfection stored at -20^{o}C for further uses.

Construction of plasmid for *Agrobacterium*-mediated transformation in tomato. For stable transformation and assessment of the cNHEJ and MMEJ-mediated precision gene replacement in tomatoes, we designed and cloned the gRNA expression cassettes (Supplementary file 1) using the Golden-gate cloning system as described previously[9, 15]. Two gRNA expression cassettes (gR1.HPAT3 and gR2.HPAT3 for SlHPAT3; gR1.HKT1;2 and gR2.HKT1;2 for SlHKT1;2) were used to generate two DSBs at each targeted site. The cNHEJ donors (cNJ.HPAT3-1 for SlHPAT3; cNJ.HKT1;2 for SlHKT1;2) and MMEJ donor (MJ.HPAT3-1 for SlHPAT3; MJ.HKT1;2 for SlHKT1;2) were designed to be flanked by two gRNAs (gDR1.HPAT3 and gDR2.HPAT3 for cNJ.HPAT3-1; gDR3.HPAT3-1 and gDR4.HPAT3 for MJ.HPAT3; gDR1.HKT1;2 and gDR2.HKT1;2 for cNJ.HKT1;2; gDR3.HKT1;2 and gDR4.HKT1;2 for MJ.HKT1;2) cutting sites (Supplementary file 1). The binary plasmids were constructed to test the cNHEJ and MMEJ approaches using a conventional T-DNA and a geminiviral replicon system[9]. The NptII selection marker expression cassette (pNOS-NptII-tOCS) is driven by the NOS promoter and terminated by the OCS terminator (Addgene # 51144). An intron-containing plant codon-optimized SpCas9 driven by a CaMV 35S promoter and CaMV 35S terminator (p35S-pcoCas9I-t35S) was used (Supplementary file 1).

Isolation of protoplasts. Tomato (*Solanum lycopersicum* cv. Micro-Tom*)*, lettuce (*Lactuca sativa* L. cv. Cheongchima), and cabbage (*Brassica. oleracea*) seeds were sterilized with 70% ethanol for 3 min, 1% hypochlorite solution for 15 min, and washed five times with distilled water. The sterilized seeds were inoculated in a medium containing 1/2 Murashige and Skoog salts, 0.4 mg/L thiamine HCl, 100 mg/L Myo-

inositol, 30 g/L sucrose, and 8 g/L gelrite, pH 5.7. The seedlings were grown in a growth chamber under a 16 h light/8 h dark photoperiod (100–130 μmol/m^2 s) at 25°C for tomato and 20°C for lettuce, and 23°C for cabbage.

For protoplast isolation of tomato and cabbage, the cotyledons of 4-day-old tomato seedlings and the cotyledons of 7-day-old cabbage seedlings were immersed in cell and protoplast washing solution (CPW) containing 0.5% cellulase (Novozymes, Basgsvaerd, Denmark), 0.5% pectinase (Novozymes), 1% viscozyme (Novozymes), 3 mM MES (pH 5.8) and 9% mannitol. After 15 min of vacuum infiltration, the suspension was incubated for 2-4 hr on a rotary shaker at 50 rpm at 25°C. The suspension was filtered through an eight-layer gauze and centrifuged for 5 min at 100 *g*. Protoplasts were separated on a 21% sucrose density gradient and then collected at the interface of W5 solution (2 mM MES pH 5.8, 154 mM NaCl, 125 mM $CaCl_2$, 5 mM KCl). The harvested protoplasts were washed three times with W5 solution and then resuspended in MMG solution (4 mM MES pH 5.7, 0.4 M mannitol, 15 mM $MgCl_2$). The concentration of protoplasts was determined using a hemocytometer.

For the lettuce protoplast isolation, the cotyledons of 7 d-old seedlings were digested with 10 mL of enzyme solution (1% [w/v] Viscozyme (Novozyme), 0.5% Celluclast (Novozyme), and 0.5% Pectinex (Novozyme), 3 mM MES (2-[N-Morpholino] ethanesulfonic acid), pH 5.7 and 9% mannitol in CPW salts with shaking at 40 rpm for 4–6 h at 25 °C in the dark. The protoplast mixture was then filtered through a 40 μm nylon cell strainer (Falcon) and collected by centrifugation at 800 rpm for 5 min in a 14 mL round tube (SPL). The collected protoplasts were re-suspended in W5 solution (2 mM MES [pH 5.7], 154 mM NaCl, 125 mM $CaCl_2$, and 5 mM KCl) and further centrifuged at 800 rpm for 5 min. Finally, the protoplasts were re-suspended in W5 solution and counted under a microscope using a hemocytometer. Protoplasts were adjusted to a density of 1×10^6/mL in MMG solution before transfection. The transfected protoplasts were cultured in protoplast culture medium (MS medium containing 0.4 mg/L thiamine HCl, 100 mg/L myo-inositol, 30 g/L sucrose, 0.2 mg/L 2,4-dichlorophenoxyacetic acid [2,4-D], and 0.3 mg/L 6-benzylaminopurine [BAP], pH 5.7) in the dark f at 25°C for 4 weeks.

PEG-mediated RNP and donor transfections. SpCas9 protein was purchased from ToolGen, Inc. (South Korea), and guide RNAs were synthesized by GeneArt Precision gRNA Synthesis Kit (Invitrogen) according to the manufacturer's protocol. PEG-mediated RNP and donor transfections were performed in the previous study[16].

For ribonucleoprotein (RNP) and donor DNA transfections with tomato and cabbage protoplasts, 2×10^5 protoplasts were transfected with the purified SpCas9 protein (20 μg) premixed with *in vitro*-transcribed sgRNA 1 (10 μg), sgRNA 2 (10 μg), and donor templates (300 pmol) in PBS buffer followed by incubating for 10 min at 25°C. The RNP complexes were mixed with protoplasts and then supplemented with an equal volume of 40% PEG transfection solution (40% PEG 4000, 0.2 M mannitol, and 0.1 M $CaCl_2$). This suspension was mixed gently and then incubated at room temperature for 10 min. An equal volume of W5 solution was added for washing, followed by centrifugation at 100 *g* for 5 min. The supernatant was discarded, and the protoplasts were incubated with 1 ml of W5 solution in the dark at 25°C for 48 h. Afterwards, the cells were collected for gDNA isolation and subsequent targeted deep sequencing analysis.

For lettuce protoplast transfection, SpCas9 protein and sgRNAs were premixed in 1× NEB buffer 3 for at least 10 minutes at room temperature and 2×10^5 protoplast cells were transfected with SpCas9 protein (20 μg) premixed with sgRNAs (10 μg each) and donor DNA (300 pmol). A mixture of 2×10^5 protoplast cells was re-suspended in 200 μl MMG solution and then was slowly mixed with RNP complex, donor, and 350 μl of PEG solution (40% [w/v] PEG 4000, 0.2 M mannitol, and 0.1 M CaCl2). After incubation for 10 min, the transfected protoplast cells were gently re-suspended in 650 μL W5 solution. After additional incubation for 10 min, 650 μL W5 solution was added slowly again and was mixed well by inverting the tube. Protoplasts were pelleted by centrifugation at 556 rpm for 5 min and washed gently in 1 ml W5 solution. Protoplasts were pelleted by centrifugation at 556 rpm for 5 min and re-suspended gently in 1 ml WI solution (4 mM MES [pH 5.7], 0.5 M mannitol, and 20 mM KCl). Finally, the protoplasts were transferred into a 60 × 15 mm petri dish (Falcon), cultured under dark conditions at 25°C for 48 h and then analyzed for genome editing efficiency.

Agrobacterium-mediated tomato transformation. The Agrobacterium-mediated tomato transformation was conducted using a protocol published by Vu and coworkers [9] with or without 1 µM NU7441 treatment for 5 days post-washing. Ten-day post-transformation, thirty cotyledon fragments were collected per transformation plate to isolate genomic DNAs and subsequent miniseq analysis. Regenerated plants were selected in media containing 100 mg/L kanamycin and transferred to soil pots before analyzing for the editing performance. Genomic DNAs were extracted from the plants and analyzed by PCR amplification of the targeted sequences and by Sanger sequencing.

Targeted deep sequencing. Genomic DNAs were isolated from the protoplasts using the CTAB method. We used the miniseq sequencing service (MiniSeqTM System, Illumina, USA) to obtain targeted deep sequencing of the edited genomic sites. Miniseq samples were prepared in three PCRs according to the manufacturer's guidelines, with genomic DNAs as the first PCR template. The first and second PCRs used primer listed in Supplementary Table 1, whereas the third PCRs were conducted with the manufacturer's primers to assign a sample ID. A high-fidelity DNA Taq polymerase (Phusion, NEB, USA) was used for the PCRs. The miniseq raw data FASTQ files were analyzed using the Cas-Analyzer tool[17]. The indel analyzing window was set at 5 bases with a comparison range that covered both the read ends. A similar analysis was conducted for the targeted base changes of lettuce and cabbage genes.

Statistical analysis. The editing data, statistical analysis, and plots were further processed by the MS Excel and Graphpad Prism 9.0 programs and are explained in detail in the legends of figures and tables wherever applicable.

References

1. Sakuma, T.et al. MMEJ-assisted gene knock-in using TALENs and CRISPR-Cas9 with the PITCh systems. *Nat Protoc* **11**, 118-133 (2016).
2. Yao, X. et al. CRISPR/Cas9 - Mediated Precise Targeted Integration In Vivo Using a Double Cut Donor with Short Homology Arms. *EBioMedicine* **20**, 19-26 (2017).
3. Lu, Y. et al. Targeted, efficient sequence insertion and replacement in rice. *Nat Biotechnol* **38**, 1402-1407 (2020).
4. Van Vu, T. et al. CRISPR/Cas-based precision genome editing via microhomology-mediated end joining. *Plant Biotechnol J* (2020).
5. Nakade, S. et al. Microhomology-mediated end-joining-dependent integration of donor DNA in cells and animals using TALENs and CRISPR/Cas9. *Nat Commun* **5**, 5560 (2014).

6. Ata, H. et al. Robust activation of microhomology-mediated end joining for precision gene editing applications. *PLoS Genet* **14**, e1007652 (2018).
7. Bae, S., Kweon, J., Kim, H.S. & Kim, J.S. Microhomology-based choice of Cas9 nuclease target sites. *Nat Methods* **11**, 705-706 (2014).
8. Dutta, A. et al. Microhomology-mediated end joining is activated in irradiated human cells due to phosphorylation-dependent formation of the XRCC1 repair complex. *Nucleic Acids Res* **45**, 2585-2599 (2017).
9. Vu, T.V. et al. Highly efficient homology-directed repair using CRISPR/Cpf1-geminiviral replicon in tomato. *Plant Biotechnol J* (2020).
10. Li, X.M. et al. Natural alleles of a proteasome alpha2 subunit gene contribute to thermotolerance and adaptation of African rice. *Nat Genet* **47**, 827-833 (2015).
11. Yuan, H. et al. A Single Amino Acid Substitution in an ORANGE Protein Promotes Carotenoid Overaccumulation in Arabidopsis. *Plant Physiol* **169**, 421-431 (2015).
12. Yazdani, M. et al. Ectopic expression of ORANGE promotes carotenoid accumulation and fruit development in tomato. *Plant Biotechnol J* **17**, 33-49 (2019).
13. Mazur, B.J., Chui, C.F. & Smith, J.K. Isolation and characterization of plant genes coding for acetolactate synthase, the target enzyme for two classes of herbicides. *Plant Physiol* **85**, 1110-1117 (1987).
14. Brooks, C.et al. Efficient gene editing in tomato in the first generation using the clustered regularly interspaced short palindromic repeats/CRISPR-associated9 system. *Plant Physiol* **166**, 1292-1297 (2014).
15. Vu, T.V. et al. Improvement of the LbCas12a-crRNA system for efficient gene targeting in plants. *Research Square* (2021).
16. Woo, J.W. et al. DNA-free genome editing in plants with preassembled CRISPR-Cas9 ribonucleoproteins. *Nat Biotechnol* **33**, 1162-1164 (2015).
17. Park, J.et al. Cas-analyzer: an online tool for assessing genome editing results using NGS data. *Bioinformatics* **33**, 286-288 (2016).

Acknowledgments

This work was supported by the National Research Foundation of Korea (Grant NRF 2020R1I1A1A01072130, 2020M3A9I4038352, 2020R1A6A1A03044344, 2021R1A5A8029490, 2022R1A2C3010331) and the Program for New Plant Breeding Techniques (NBT, Grant PJ01478401), Rural Development Administration (RDA), Korea.

Author contributions

Conceptualization, T.V. V and J.Y.K.; Methodology, T.V. V and J.Y.K.; Conducted experiments, T.V. V., G.H.L, S.H.C, J.Y.M., S.W.K., J.C.J, N.T.N, S.D., M.T.T., Y.W.S, J.K, Y.J.S; Data analysis, T.V. V. and J.Y.K.; Writing – Original Draft, T.V. V.; Writing – Review & Editing, T.V. V. and J.Y.K.; Funding Acquisition, T.V.V., and J.Y.K.; and Supervision, T.V. V and J.Y.K.

Competing interests

The authors have applied for Korean patents (10-2021-0089814) and PCT patents (PCT-KR2021-008727) based on the results reported in this paper.

Figure Legend

Fig. 1. HR-independent precision editing approaches using CRISPR/SpCas9. a, Schematic diagrams of cNHEJ- and MMEJ-mediated gene editing of tomato targeted loci SlHPAT3 using donor sense sequences (cNJ.HPAT3-1, MJ.HPAT3-1, MJ.HPAT3-2, and MJ.HPAT3-3). Exons are drawn as blue boxes, and the discontinuous lines in each gene represent intron parts of the gene; The expected cutting sites (3-nt upstream of a PAM) of gRNAs are indicated by black scissors; the intended base changes (A1, A2, B, C, D1, and D2) are painted in the red font that is denoted by the discontinuous red boxes. The diagrams are not drawn to scale. **b**, Editing frequency of respective repaired products/alleles revealed from miniseq data. **c**, Editing efficiency revealed by targeted deep sequencing data of the various donor doses. **d**, editing efficiencies revealed by the treatment of donors with different microhomology lengths. **e**, Editing efficiency revealed from targeted deep sequencing data of the treatments at different NU7441 concentrations. **f**, The detailed targeted deep sequencing data analyzed with the various NU7441 concentrations and microhomology lengths. Targeted editing efficiency is the sum of the precise editing efficiency and the only B and C editing efficiency. Precise editing efficiency was calculated by dividing total reads containing all the base changes by the total reads. The only B and C editing efficiency were calculated by dividing total reads containing only B and C base changes by the total reads. One-sided editing efficiency was calculated by dividing total reads containing only either the left-sided bases (A1 and A2) or the right-sided base pairs (D1 and D2) by the total reads.

Fig. 2. MMEJ-mediated precision gene editing in lettuce and cabbage. a-b, Schematic diagrams of targeted loci (TT1, Or, and ALS1 with their GenBank accession number), targeted sequences, gRNA binding sites, and MMEJ donors in lettuce (**a**) and cabbage (**b**). The Exons are drawn as colored boxes (purple boxes with lettuce's loci and pink boxes for cabbage), and the discontinuous line in each gene

represents intron parts of the gene. The expected cutting sites (3-nt upstream of a PAM) of the gRNAs are indicated with the black scissors; the intended base changes are painted in the red font; the targeted amino acid changes and corresponding triplexes are denoted by the discontinuous red boxes, and the texts placed on their top. The diagrams are not drawn to their scales. **c**, MMEJ-mediated editing efficiency in lettuce at the TT1, Or, and ALS1 loci. **d**, MMEJ-mediated editing efficiency in cabbage at the TT1, Or, and ALS1 loci.

Supplementary item

Supplementary figure legends

Supplementary Fig. 1. HR-independent strategies for precision gene/allele replacement using CRISPR/SpCas9

Supplementary Fig. 2. HR-independent precision editing approaches using CRISPR/SpCas9

Supplementary Fig. 3. Sanger sequencing data revealed precise replacement of DNA by MMEJ donor

Supplementary Fig. 4. Indel alleles revealed from transfection of SpCas9, gR1.HPAT1 and gR2.HPAT3 with cNJ.HPAT3-1 donor

Supplementary Fig. 5. Indel alleles revealed from transfection of SpCas9, gR1.HPAT1 and gR2.HPAT3 with MJ.HPAT3-1 donor

Supplementary Fig. 6. The frequency of the MMEJ-mediated repaired products at different donor doses

Supplementary Fig. 7. Agrobacterium-mediated system for cNHEJ and MMEJ-mediated gene editing in tomato

Supplementary Fig. 8. Representative repaired products obtained by the pMJ1 and pMJ2 vector.

Supplementary Tables

Supplementary Table 11. Data revealed from the targeted deep-sequencing analysis of MMEJ-mediated editing in lettuce

Supplementary Table 12. Data revealed from the targeted deep-sequencing analysis of MMEJ-mediated editing in cabbage

Supplementary files

Supplementary file 1: Sequences used in the study

Fig. 1

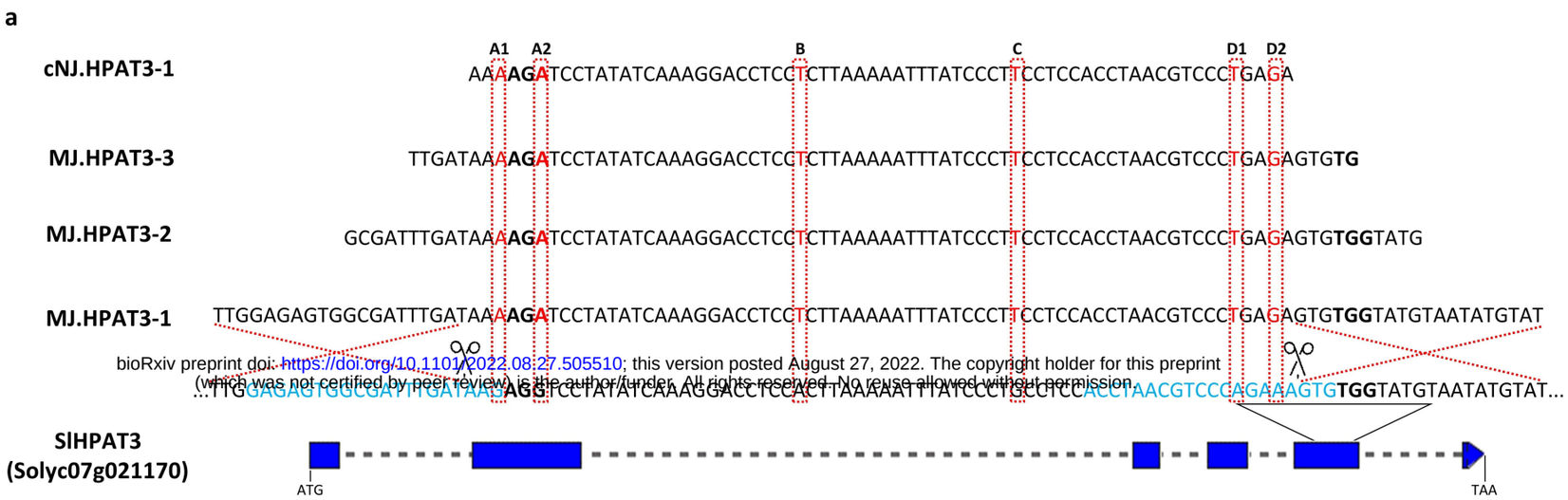

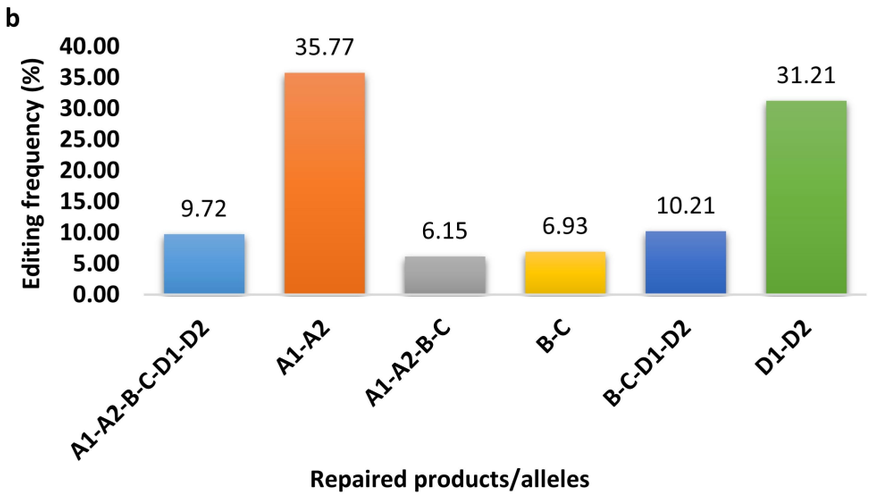

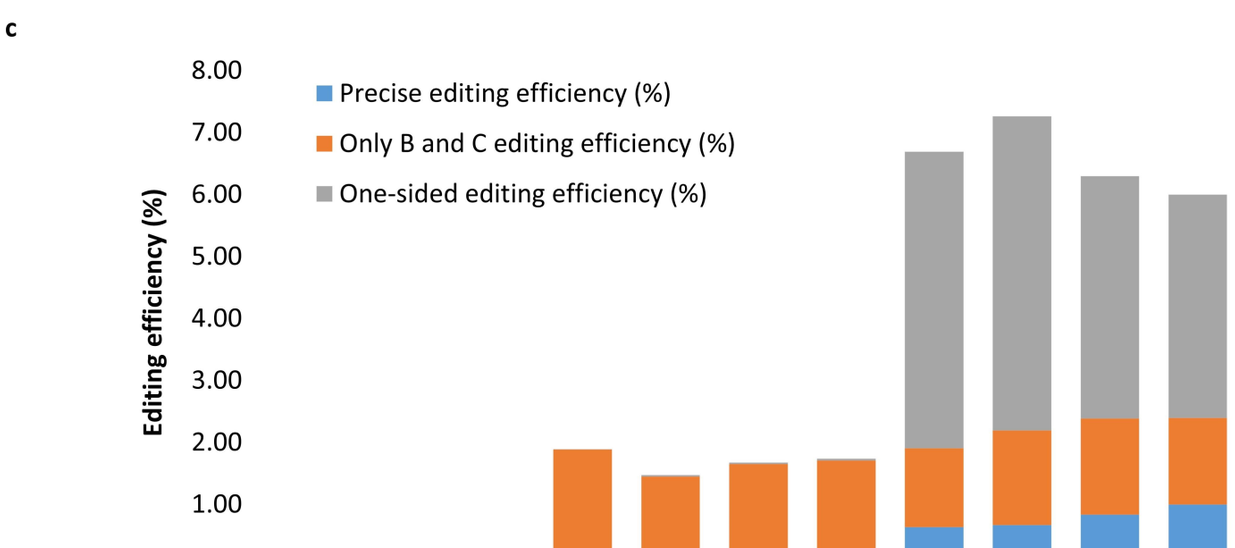

Treatment	1	2	3	4	5	6	7	8	9	10	11
SpCas9	+	+	+	+	+	+	+	+	+	+	+
gR1.HPAT3	+	-	+	+	+	+	+	+	+	+	+
gR2.HPAT3	-	+	+	+	+	+	+	+	+	+	+
Donor dose (pmol)	-	-	-	50	100	200	300	50	100	200	300
Donor	-	-	-		cNJ.HPAT3-1				MJ.HPAT3-1		

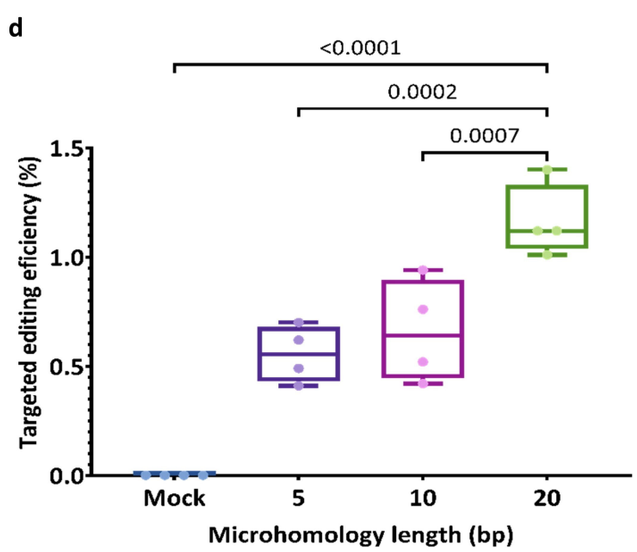

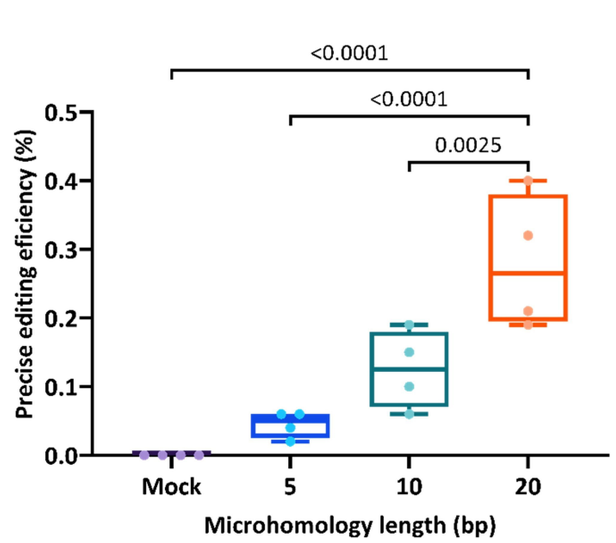

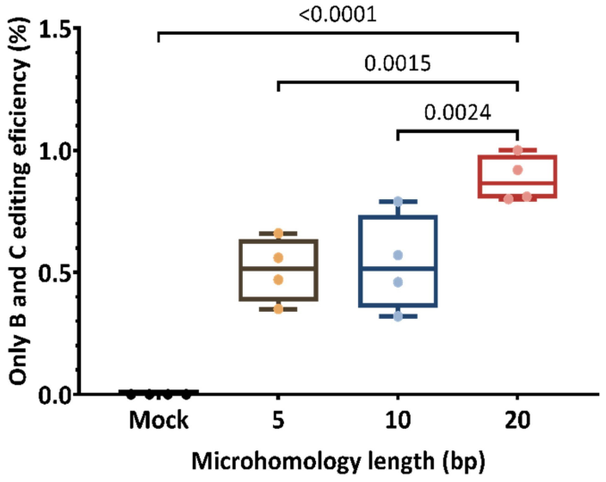

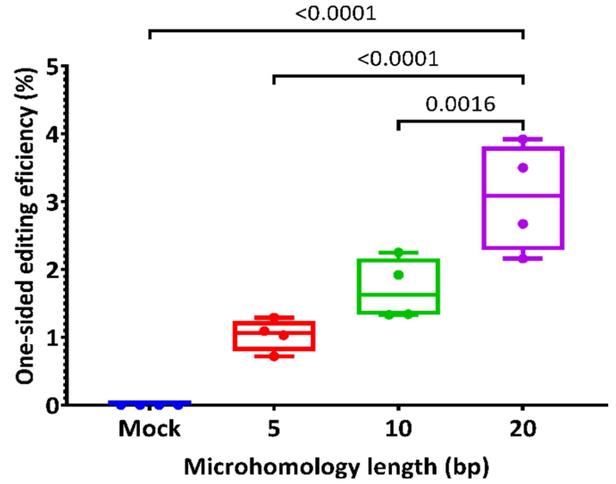

e

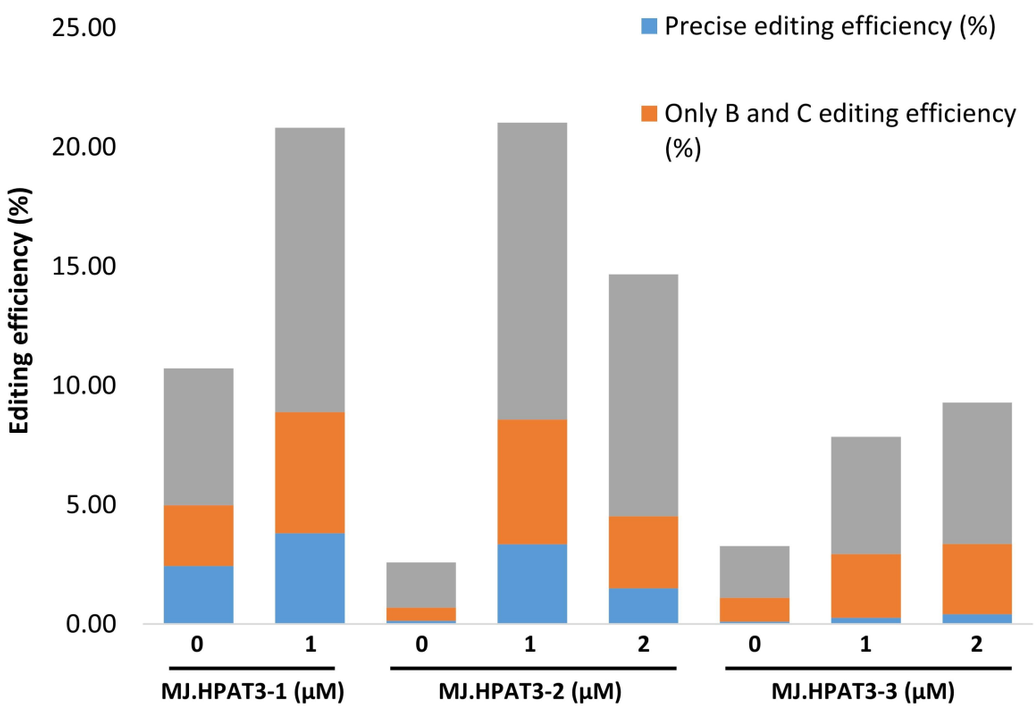

f

No.	Donor	Nu7441 (μM)	Total reads	Total editing efficiency (%)	Precise editing efficiency (%)	Only B and C editing efficiency (%)	One-sided editing efficiency (%)	gR1.HPAT3 indel rate (%)	gR2. HPAT3 indel rate (%)
1	cNJ.HPAT3-1	0.0	72024	0.84	0.00	0.84	0.00	0.01	0.01
2		0.5	69595	0.84	0.00	0.84	0.00	0.01	0.01
3		1.0	69595	1.32	0.00	1.32	0.00	0.02	0.02
4		2.0	62798	1.58	0.00	1.58	0.00	0.20	0.19
5	MJ.HPAT3-1	0.0	18363	13.16	2.44	2.54	5.73	1.08	1.03
6		1.0	27496	24.61	3.80	5.09	11.91	3.32	3.54
7	MJ.HPAT3-2	0.0	56735	2.72	0.14	0.55	1.90	0.97	0.95
8		1.0	47518	24.35	3.34	5.24	12.44	1.19	1.13
9		2.0	77234	16.17	1.50	3.01	10.15	0.72	0.74
10	MJ.HPAT3-3	0.0	72885	3.37	0.10	1.00	2.18	0.16	0.14
11		1.0	77561	8.11	0.26	2.68	4.91	0.33	0.25
12		2.0	61072	9.70	0.41	2.94	5.94	0.38	0.31

Fig. 2

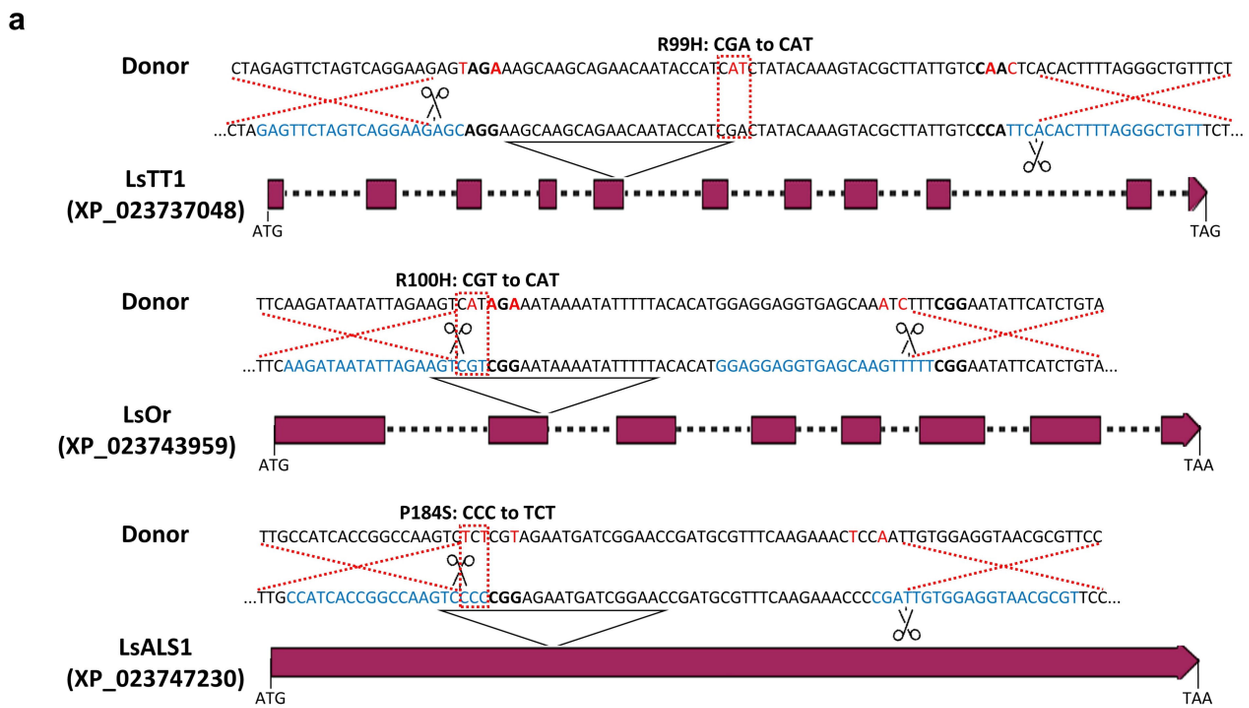

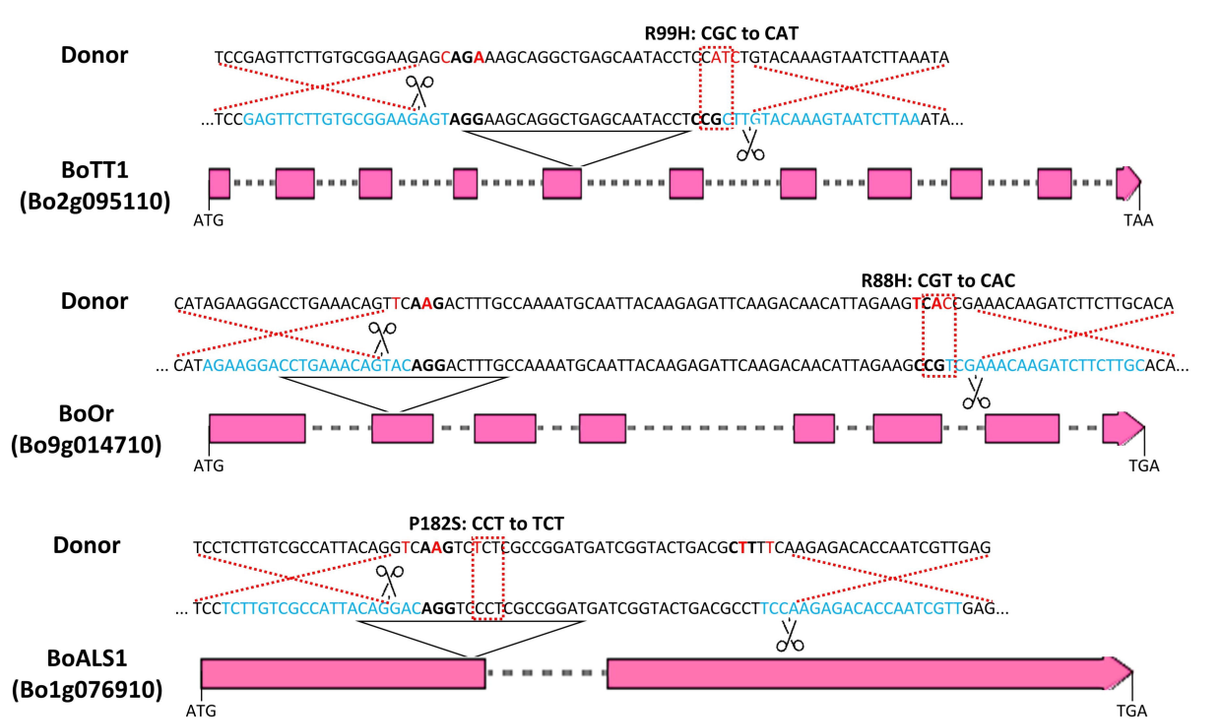

c

No.	Locus	Accession	Total reads	Targeted editing efficiency (%)	Precise editing efficiency (%)	gRNA1 indel rate (%)	gRNA2 indel rate (%)
1	LsTT1	XP_023737048	96871	0.78 ± 0.30	0.000	0.87 ± 0.71	0.35 ± 0.27
2	LsOr	XP_023743959	90601	0.42 ± 0.27	0.13 ± 0.10	1.07 ± 0.71	0.94 ± 0.39
3	LsALS1	XP_023747230	89394	4.47 ± 1.98	1.81 ± 0.75	2.69 ± 1.19	2.15 ± 0.99

d

No.	Locus	Accession	Total reads	Targeted editing efficiency (%)	Precise editing efficiency (%)	gRNA1 indel rate (%)	gRNA2 indel rate (%)
1	BoTT1	Bo2g095110	16905	7.27 ± 4.46	1.71 ± 0.48	4.83 ± 1.27	2.39 ± 1.20
2	BoOr	Bo9g014710	68028	3.94 ± 0.14	1.56 ± 0.65	24.37 ± 1.99	16.76 ± 6.12
3	BoALS1	Bo1g076910	90366	2.51 ± 1.19	0.73 ± 0.35	1.13 ± 0.40	10.61 ± 5.11